Research Square

Preprints are preliminary reports that have not undergone peer review.
They should not be considered conclusive, used to inform clinical practice,
or referenced by the media as validated information.

Predicting Somatosensory Awareness from Intracranially Informed Scalp EEG

Andrea Pigorini

andreapigorini@gmail.com

Universty of Milan https://orcid.org/0000-0002-1856-3413

Alessandra Calcagno

Universty of Milan

Francesca Mannini

Universty of Milan

Ezequiel Mikulan

University of Milan https://orcid.org/0000-0001-7259-6120

Alice Rossi Sebastiano

University of Turin

Angela Comanducci

University of Milan

Gabriel Hassan

University of Milan

Flavia Maria Zauli

University of Milan https://orcid.org/0000-0002-7328-6068

Maria Del Vecchio

National Research Council of Italy

Pietro Avanzini

Istituto di Neuroscienze, Consiglio Nazionale delle Ricerche https://orcid.org/0000-0001-9371-451X

Ivana Sartori

Ospedale Niguarda Ca' Granda https://orcid.org/0000-0001-5659-0730

Francesca Garbarini

University of Turin https://orcid.org/0000-0003-1210-0175

Article

Keywords: Conscious somatosensory perception, simultaneous hdEEG–SEEG recordings, intracerebral tonic activity, median nerve stimulation, machine learning

Posted Date: October 5th, 2026

DOI: https://doi.org/10.21203/rs.3.rs-11143622/v1

License: This work is licensed under a Creative Commons Attribution 4.0 International License.
Read Full License

Additional Declarations: There is **NO** Competing Interest.

Abstract

Behavioural reports are the standard means of determining whether a stimulus is consciously perceived, but assessing perception when patients are unable to provide such reports remains challenging. Here, using a machine-learning approach trained on simultaneous high-density scalp and intracranial EEG recordings during median nerve stimulation, we derived a candidate non-invasive marker of somatosensory awareness by predicting from scalp EEG the intracranial tonic operculo-insular response previously associated with conscious somatosensory perception. In an independent multicentre perceptual-threshold dataset of healthy participants, the scalp estimate of tonic activity was larger for perceived than unperceived stimuli and consistently distinguished the two conditions at the individual level. This participant-level consistency was not observed for the Somatosensory Awareness Negativity, the best-established scalp EEG marker of somatosensory awareness. Moreover, a decision threshold derived from the perceptual dataset generalized without recalibration to a third, independent dataset, separating wakefulness from deep NREM sleep across all participants despite the absence of concurrent perceptual reports. Thus, our approach identifies an intracranially informed, non-invasive EEG marker associated with conscious somatosensory processing that generalizes across individuals, datasets and brain states, supporting its future evaluation in clinical settings where behavioural reports are unavailable.

INTRODUCTION

Research on the neural correlates of consciousness has identified numerous electrophysiological signatures associated with conscious perception[1–4]. These signatures have been characterized using non-invasive approaches, such as EEG[5,6] and MEG[7,8], as well as invasive intracranial recordings[9–11], which provide access to neural dynamics at markedly different spatial scales and with different sampling characteristics compared with non-invasive methods[12,13]. However, these findings failed to provide non-invasive markers of conscious perception that are reliable at the individual subject level[4,14,15], at the same time reflecting the engagement of specific awareness-related neural dynamics without relying on behavioural report[16,17].

Somatosensory perception provides a well-documented scenario for testing the reliability of non-invasive biomarkers of conscious perception. Peripheral nerve stimulation has long been known to evoke a contralateral frontocentral negativity around 120–180 ms, historically labelled as the N140[18,19]. Subsequent studies showed that this component is enhanced when somatosensory stimuli are consciously perceived[20], leading to its more recent reframing as the Somatosensory Awareness Negativity (SAN), paralleling analogous modality-specific negativities described within the broader Perceptual Awareness Negativity (PAN) framework[21]. However, SAN latency, morphology and amplitude vary substantially across individuals[22–24], limiting its reliability as an individual subject level marker of conscious perception.

Stereo-electroencephalography (SEEG) studies have provided insights into the intracranial dynamics associated with the SAN. Early phasic responses, possibly corresponding to the scalp N20, primarily reflect afferent processing, vanish within ~ 50 ms after stimulation and can remain detectable in the absence of conscious perception (e.g. in anesthesia or coma patients), making them unlikely to account for the later SAN[20,25–27]. They are followed by sustained broadband gamma activity in operculo-insular regions lasting over 200 ms[27]. This tonic activity is distributed bilaterally[28], emerges around perceptual threshold, distinguishes perceived from unperceived stimuli, and is preserved even when participants are not required to report their perceptual experience, supporting its association with conscious perception rather than overt reporting[29].

Simultaneous intracranial and scalp recordings provide a powerful framework for linking the spatiotemporal specificity of invasive electrophysiology with the accessibility of non-invasive EEG[30]. Using this approach, we recently showed that the scalp SAN is temporally associated with sustained operculo-insular activity, whose local broadband gamma activity is followed by a deflection of the local field-potential, which is aligned with the scalp negativity (Mikulan et al., in preparation). Importantly, simultaneous scalp–intracranial recordings can also be used to learn predictive mappings between non-invasive and invasive signals, including during spontaneous brain activity[31,32].

Given the premises above, here we wondered whether applying machine-learning on simultaneous high-density EEG (hdEEG) and SEEG recordings during median nerve stimulation could extract from scalp EEG an intracranially informed feature of the tonic response that, despite resembling the SAN, could mitigate its inter-individual variability, thus providing a more reliable and generalizable index of somatosensory awareness. Once the tool was established, in the present study we tested its generalizability across participants, centres, acquisition systems, stimulation intensities and experimental protocols. Finally, we examined its robustness across markedly different brain states, using wakefulness and deep NREM sleep as a physiological use case to explore its potential future translation to bedside assessment in patients who cannot communicate.

RESULTS

We leveraged simultaneous hdEEG–SEEG recordings combined with a machine-learning approach to derive a non-invasive estimate of the operculo-insular tonic response to median nerve stimulation associated with somatosensory conscious perception. Specifically, a time-delayed ridge-regression model[33–35] was trained to predict the time-resolved intracranial response from scalp hdEEG and evaluated in held-out participants using leave-one-subject-out cross-validation.

For subsequent scalp-only analyses, we operationally defined Scalp Estimated Tonicity (SET) as the area under the predicted tonic-response waveform exceeding twice the prestimulus baseline standard deviation between 60 and 250 ms. The model and SET quantification were then applied, without adaptation or recalibration, to an independent multicentre perceptual-threshold dataset, where trial-by-trial reports allowed us to test whether SET reliably distinguished perceived from unperceived stimuli at

the individual-subject level and to compare its performance with the conventional SAN. We subsequently used this dataset to derive a SET decision threshold (SET*), which was finally applied, together with the unchanged model, to an independent wake–N3 sleep dataset acquired without concurrent perceptual reports, providing a further test of generalization across brain states.

Scalp EEG predicts intracranial tonic responses in held-out participants

As a first step of analysis, we trained a ridge-regression model to predict intracranial tonic responses from the scalp EEG. We trained the model on simultaneously recorded hdEEG and SEEG (Fig. 1a, see Methods). After training, the optimal time-delayed ridge regression model had an alpha value of 100 and a minimum temporal lag of 0 ms and a maximum lag of 40 ms.

Prediction performance was quantified by correlating each model-predicted waveform with the corresponding observed intracranial tonic-response waveform, taking the maximum Pearson correlation across temporal lags of up to ± 50 ms. In leave-one-subject-out cross-validation, the median maximum correlation across pseudo-trials from held-out participants was 0.67 (interquartile range [IQR] = 0.55–0.75). After aggregating predictions within each participant, the median correlation was 0.61 (IQR = 0.48–0.84).

The model therefore recovered a substantial portion of the temporal structure of the intracranial response in participants whose data had not been used for model fitting. Prediction performance nevertheless varied across participants, with median cross-validated correlations ranging from 0.28 to 0.79 (median = 0.64, IQR = 0.48–0.73), indicating interindividual differences in the strength or scalp expression of the intracranial tonic response. Figure 1b shows the observed and predicted intracranial responses averaged across held-out participants. Both waveforms displayed a delayed increase after median nerve stimulation followed by a sustained response over the subsequent post-stimulus interval.

The sensor-space distribution of the model coefficients showed its strongest contributions over frontocentral electrodes, including AF3, F2, F4 and FC2. Following alignment to a common stimulation side, the topography (Fig. 1c) was broadly compatible with the frontocentral distribution expected for the SAN[22–24] .

(a) Schematic of the recording setup and of the Time-Delayed Ridge model (see methods). **(b)** Comparison between observed and predicted tonic responses across subjects (mean ± SEM), together with the median maximum cross-correlation across pseudo-trials from held-out participants (0.67) and the median participant-level correlation (0.61). **(c)** Topographical distribution of Time-Delayed Ridge model weights from the temporal window selected for the final model (0–40 ms), averaged across temporal lags and projected onto sensor space using a 64-channel BioSemi EEG montage.

.

Both SAN and SET distinguish perceived from unperceived stimuli at the group level, but only SET provides consistent individual-level separation

The multicenter perceptual-threshold dataset included 16 participants, eight recorded in Milan and eight in Turin. On average, participants purported as perceived 48% of the stimuli (52% unperceived). The mean number of retained trials was 115 for the perceived condition and 125 for the unperceived condition. The average responses obtained in perceived and unperceived conditions from one representative subject are shown in Fig. 2b. In line with previous literature[22–24], at the group level, grand-average scalp responses differed between perceived and unperceived stimuli within the expected latency range of the SAN (Fig. 2c). Specifically, cluster-based permutation analysis identified a significant temporal cluster extending from 125 to 230 ms after stimulation, with a scalp distribution consistent with previous reports and a maximum negativity over the contralateral C6 electrode[22–24]. Within this interval, perceived stimuli elicited a more negative response than unperceived stimuli. Mean amplitude of SAN was − 0.655 ± 0.439 μV in the perceived condition and − 0.313 ± 0.288 μV in the unperceived condition and the difference between the two conditions was significant across subjects (Wilcoxon signed-rank test: $W = 18$, $p = 0.0076$; $d_z = -0.760$), confirming that the SAN contained reliable information about somatosensory perception when responses were aggregated across participants (Fig. 2d).

However, individual waveforms showed substantial variability in the latency, amplitude, and morphology of the SAN. A clearly identifiable negative component was present in some participants, whereas in others it was small, temporally dispersed, or not readily distinguishable from background activity (see Supplementary figure S2). Consequently, despite the significant group-level effect, the within-participant difference in N140 amplitude between perceived and unperceived condition averages was heterogeneous and did not show a consistent pattern across individuals (Fig. 2d).

We then applied the model trained on simultaneous hdEEG–SEEG recordings to the same multicenter dataset. For each participant and condition, the model generated a predicted tonic response, from which the SET was computed as the area under the curve (Fig. 2e, see methods). At the group level, SET was markedly larger for perceived than for unperceived stimuli (Fig. 2f). Mean SET was 9.93 ± 3.63 z in the perceived condition and 1.93 ± 1.94 z in the unperceived condition. This difference was significant (Wilcoxon signed-rank test: $W = 0$, $p = 3.05 \times 10^{-5}$; $d_z = 1.89$; Fig. 2g).

Unlike scalp SAN, SET also provided clear participant-level separation between conditions. Using a Leave-One-Out Cross-Validation (LOOCV) procedure, a participant-independent decision threshold (SET*) was derived from the development set. The optimal thresholds obtained across the 16 iterations were highly consistent (median SET* = 6.0, mean = 6.01 ± 0.03, range = 6.0–6.1), with LOOCV classification yielding an accuracy of 0.969 (31/32 correctly classified samples). The final SET* threshold (6.0), shown by the red dashed line in Fig. 2g, was then applied to the entire perceptual-threshold dataset. All 16 perceived-condition averages were classified as displaying estimated tonic activity, whereas all 16 unperceived-condition averages were classified as not displaying predicted tonic activity, resulting in

complete development-set separation (overall accuracy of 1, with both sensitivity and specificity equal to 1). Within each participant, the perceived and unperceived condition averages were correctly separated: SET was equal to or greater than SET* for perceived stimuli and below SET* for unperceived stimuli.

(a) Schematic representation of the somatosensory perceptual-threshold paradigm. Participants received 250 constant-intensity median nerve stimuli set close to their individual perceptual threshold. Each trial comprised a jittered prestimulus interval (1.5 ± 0.25 s), median nerve stimulation, a 0.5-s post-stimulus interval, and a visual cue prompting a perceived/unperceived response. **(b)** Single-participant example of scalp EEG responses (Nave indicates the number of trials averaged per condition) to perceived and unperceived stimuli, with channel C6 highlighted in black. **(c)** One-sample cluster-based permutation test (PCT) performed on the within-participant difference waveforms at channel C6. A significant negative cluster was identified between 0.125 and 0.230 s after stimulation, corresponding to the N140 component and highlighted in light green. The top-right panel shows the scalp distribution of the perceived-minus-unperceived difference averaged across the significant temporal cluster, revealing the expected contralateral frontocentral negativity centred over electrode C6. **(d)** Comparison of SAN amplitude between perceived and unperceived conditions. At the group level, SAN amplitude was significantly larger, i.e. more negative, for perceived than for unperceived stimuli (**p < 0.01). **(e)** Representative examples of the tonic responses predicted for the perceived and unperceived conditions, corresponding to the scalp EEG signals shown in panel B. Scalp Estimated Tonicity (SET) was quantified between 60 and 250 ms as the time integral of estimated waveform exceeding a predefined baseline-exceedance criterion of 2 × σbaseline, indicated by the dashed line. **(f)** One-sample cluster-based permutation test performed on the within-participant difference between the estimated waveforms obtained for perceived and unperceived conditions. **(g)** Comparison of SET values between perceived and unperceived conditions. At the group level, SET was significantly higher for perceived than for unperceived stimuli (**p < 0.01). The SET decision threshold derived from the pooled perceptual dataset (SET = 6; red dashed line) achieved complete development-set separation between perceived and unperceived condition averages (accuracy = 1).

Estimated tonic activity is reduced during deep NREM sleep with respect to wakefulness

The trained model was subsequently applied to the independent wake–sleep dataset using the same SET quantification procedure employed in the perceptual-threshold dataset. The model was not retrained, and SET* = 6, previously derived from the pooled perceptual dataset, was applied without recalibration.

SET was substantially larger during wakefulness than during sleep. Mean SET was 23.4 ± 9 during wakefulness and 0.3 ± 0.4 during sleep. The within-participant difference was significant (Wilcoxon signed-rank test: W = 0, p = 0.0078) and was associated with a large effect size (dz = 2.65).

Application of SET* classified all eight wake-condition averages as displaying estimated tonic activity, and all eight sleep-condition averages were classified as not displaying estimated tonic activity. Overall, 16 out of 16 condition averages were correctly classified, corresponding to a perfect accuracy of 1. Notably, the model had not been trained to distinguish vigilance states and SET* had been derived from the independent near-threshold perceptual dataset. These findings demonstrate that SET* generalized to the wake–sleep contrast without recalibration.

Importantly, prediction performance improved as the number of selected trials per subject increased (Fig. 3f). Specifically, classification accuracy increased from 0.625 using 5 trials to 1 using 55 trials, after which performance reached a plateau, indicating that reliable discrimination between wake and sleep can be achieved with approximately 55 trials per participant.

(a) Scalp EEG responses recorded during wakefulness (Nave = 250) in one representative subject. **(b)** Corresponding estimated scalp activity, yielding a SET value of 15. **(c)** Scalp EEG responses recorded during sleep (Nave = 188) in the same subject of (a). **(d)** Corresponding estimated scalp activity, yielding a lower SET value of 0. **(e)** Comparison of SET values between wakefulness and sleep. SET* (red-dashed line), derived from the independent perceptual-threshold dataset and applied without recalibration, is shown by the red dashed line. All wake-condition averages and sleep-condition averages were correctly classified, yielding an overall accuracy of 1. **(f)** Classification accuracy as a function of the number of trials included in the averaged EEG response.

DISCUSSION

In the present study, we used simultaneous hdEEG–SEEG recordings to derive a non-invasive estimate of the intracranial tonic response associated with somatosensory perception. A time-delayed ridge-regression model recovered the temporal profile of this response in held-out participants and was subsequently applied, without adaptation, to two independent scalp EEG datasets. In a multicentre perceptual-threshold dataset, both the Somatosensory Awareness Negativity (SAN) and SET distinguished perceived from unperceived stimuli at the group level, but only SET consistently separated the two conditions across individuals. A decision threshold (SET*) derived from this dataset showed near-perfect leave-one-out classification and, when applied without recalibration to an independent wake–N3 sleep dataset, correctly separated all wake and sleep condition averages.

The different performance of SAN and SET may reflect the distinct information captured by the two measures. Conventional SAN quantification reduces a spatially distributed and temporally extended response to the amplitude of a negative deflection measured at a single contralateral electrode (as calculated here and in [22,23] or an ROI of electrodes, as in [36]), making it sensitive to interindividual variability in latency, morphology, source anatomy and scalp projection[22,23,37]. By contrast, SET integrates information distributed across all scalp channels and temporal delays through a transformation optimized to predict a physiologically characterized intracranial response, while also capturing its magnitude and temporal persistence above prestimulus variability. Consistently, the

frontocentral distribution of model coefficients was broadly compatible with the expected SAN topography. Nevertheless, SET should not be regarded simply as a more sensitive measure of the SAN, nor as a direct reconstruction of intracranial activity, but rather as an intracranially informed scalp-derived estimate of the tonic response.

Despite its simplicity, the time-delayed ridge-regression model proved effective in extracting participant-level information from scalp EEG. Its linear and regularized formulation is well suited to the relatively limited size of the simultaneous hdEEG–SEEG dataset and remains comparatively interpretable[34,35,38]. Larger simultaneous EEG–SEEG datasets may eventually support more complex AI-based models capable of capturing nonlinear or participant-specific relationships between scalp and intracranial activity[31,32,39]. Still, a key feature of the present approach was its ability to generalize across recording sites. Indeed, the model was successfully applied to perceptual-threshold data acquired at two centres using different EEG systems and recording environments. Although all datasets were transformed to a common montage and preprocessing framework, pooling the Milan and Turin cohorts introduced realistic between-site variability. The resulting participant-level separation suggests that model performance did not depend exclusively on acquisition-specific features of the simultaneous hdEEG–SEEG dataset. This cross-centre generalization is particularly relevant given the limited transferability that more complex deep-learning models can show across acquisition sites, a major challenge for multicentre applications[40].

The transfer to the wake–sleep dataset provided a further test of generalization, as neither the model nor SET* were developed to distinguish vigilance states and all parameters were applied without recalibration. SET was markedly higher during wakefulness and remained below threshold during N3 sleep in all participants. However, this comparison should not be interpreted as an independent validation of perceived versus unperceived classification. Conscious mentation can occur during NREM sleep[41,42], and perceptual status could not be established in the absence of trial-by-trial reports. Rather, wakefulness and stable N3 sleep provide a physiological contrast in which the likelihood of consciously perceiving the suprathreshold somatosensory stimuli is markedly different. Moreover, sleep-related changes in cortical excitability, synchrony and background EEG activity[43–46] may influence SET independently of perception.

The generalization of SET across recording conditions and brain states provides a rationale for evaluating it as a candidate bedside index of stimulus-related processing in unresponsive patients with disorders of consciousness. In this context, SET would complement established EEG paradigms such as the P300/P3b and mismatch negativity (MMN)[2,4,47]. P300/P3b paradigms, particularly in active or command-following designs, depend on target detection, attention, working memory and comprehension of instructions, making negative findings difficult to interpret in severely impaired patients[48,49]. MMN can be elicited passively, but primarily indexes the detection of violations in sensory regularities and does not by itself establish conscious perception[50,51]. By contrast, SET can be computed from the response to a passively delivered somatosensory stimulus without target identification, stimulus regularity violations

or overt responses. Behavioural reports were required here to establish its association with perception, but are not required for its computation.

SET also provides a fixed decision threshold for identifying perception-related responses at the individual level, rather than requiring a contrast between behaviourally defined conditions. This feature may be particularly useful when behavioural reports are unavailable or unreliable. However, the effects of attention and task relevance remain to be assessed in awake no-report paradigms, and a low or absent SET in patients should only be interpreted after confirming preservation of the somatosensory afferent pathway.

A distinctive feature of SET is its stimulus- and modality-specific nature. Most neurophysiological measures currently applied to unresponsive patients, including the TMS–EEG Perturbational Complexity Index[52], resting-state EEG measures of complexity[2,3,53], functional connectivity, and neuroimaging indices of large-scale network integrity[54,55], primarily characterize global brain properties or the capacity to sustain consciousness. By contrast, SET probes whether a specific somatosensory event evokes a neural pattern associated with conscious perception. A value above threshold does not prove that the stimulus was consciously perceived, but indicates the presence of the awareness-related neural pattern identified in the present datasets.

This stimulus-specific perspective may potentially extend beyond somatosensation. The SAN has been framed within the broader Perceptual Awareness Negativity (PAN) framework, which describes analogous modality-specific negativities associated with conscious perception across sensory systems[21]. Whether intracranially informed measures analogous to SET can be derived for auditory or visual perception remains to be established, but simultaneous scalp–intracranial recordings provide a framework for testing this possibility (Pigorini et al 2024). Ultimately, global measures of consciousness could be complemented by a battery of stimulus-specific indices probing how individual external events are processed across sensory modalities.

Several limitations should be acknowledged. First, the simultaneous hdEEG–SEEG dataset was relatively small, with sparse, participant-specific intracranial sampling determined by clinical requirements. Nevertheless, leave-one-subject-out validation allowed us to assess generalization across participants. Second, the model was trained in patients with epilepsy, although contacts within the seizure-onset zone or showing pathological activity were excluded[12,56], and the model transferred without adaptation to healthy participants. Third, SET* was derived and evaluated in the same perceptual dataset; therefore, the complete separation observed there reflects development-set performance rather than an unbiased estimate of sensitivity and specificity. However, leave-one-participant-out classification was near-perfect, and the fixed threshold transferred to the independent wake–sleep dataset. Fourth, analyses were based on condition averages, and the wake–sleep dataset lacked direct perceptual reports; single-trial performance and perceptual classification across brain states therefore remain to be established. Finally, only somatosensory stimulation was tested, and the effects of attention and task relevance on SET require further investigation[16].

Despite these limitations, the present study shows that distributed scalp EEG activity can be transformed into a non-invasive estimate of a physiologically characterized intracranial response. This intracranially informed measure provided more consistent participant-level discrimination than the conventional SAN and generalized across datasets, acquisition settings and physiological brain states. Following independent perceptual and clinical validation, this approach may help assess whether specific sensory events engage awareness-related cortical dynamics in individuals who cannot communicate. More broadly, our findings illustrate how simultaneous invasive and non-invasive recordings can translate intracranial physiology into subject-level scalp EEG measures with potential clinical relevance.

MATERIAL AND METHODS

Overall study design

1. Simultaneous hdEEG and SEEG recordings acquired during median nerve stimulation were used to train a time-delayed ridge-regression model to predict the time-resolved intracranial tonic response from scalp EEG activity (Fig. 1). Model generalization to participants not included during fitting was assessed using leave-one-subject-out cross-validation. For subsequent scalp-only analyses, the predicted tonic response was quantified as Scalp Estimated Tonicity (SET).
2. The trained model and SET quantification were applied without adaptation to an independent perceptual-threshold dataset combining healthy participants recorded in Milan and Turin with different EEG acquisition systems (Fig. 2). Participants reported whether each near-threshold median nerve stimulus had been perceived, allowing us to test whether SET distinguished perceived from unperceived stimuli at both the group and individual-participant levels. Performance was compared with the conventional Somatosensory Awareness Negativity (SAN) measured directly from scalp EEG. The pooled perceptual dataset was subsequently used to derive a single participant-independent SET decision threshold (SET*).
3. The same trained model, SET quantification procedure and fixed SET* were applied without retraining or recalibration to an independent wake–N3 sleep dataset acquired during suprathreshold median nerve stimulation and without concurrent perceptual reports (Fig. 3). This final analysis tested whether SET and its decision threshold generalized across markedly different physiological brain states and recording conditions.

Simultaneous hdEEG-SEEG dataset

Participants. The model-development dataset comprised eight patients undergoing SEEG monitoring as part of the presurgical evaluation of drug-resistant focal epilepsy at the Claudio Munari Epilepsy Surgery Centre, ASST Grande Ospedale Metropolitano Niguarda, Milan, Italy.

The dataset initially included 11 recording sessions because three participants underwent separate stimulation sessions involving the two upper limbs. To balance the number of sessions according to the stimulation side, the right-sided stimulation session containing the lowest number of usable trials was

excluded. The final dataset therefore comprised ten sessions, including five left-median-nerve and five right-median-nerve stimulation sessions.

SEEG implantation sites and the number of implanted electrodes were determined exclusively according to clinical requirements[57]. No electrode was implanted for research purposes. All participants provided written informed consent before participation. The experimental procedures were approved by the local ethical committee (Prot.n. 348–24062020, Niguarda Hospital, Milan, Italy) and were conducted in accordance with the Declaration of Helsinki.

Demographic and clinical information, stimulation side and the number and anatomical distribution of the retained SEEG contacts are reported in Supplementary Table S1.

Median nerve stimulation. The median nerve was electrically stimulated at the wrist using constant-current square-wave pulses delivered through surface electrodes. Individual pulses had a duration of 0.2 ms and were delivered at a fixed frequency of 1 Hz. Stimulation intensity was set to 110% of the individual motor threshold (as in Avanzini et al. 2016). Each recording session comprised approximately 500 stimuli (484.5 ± 166.8).

Simultaneous electrophysiological recordings. Scalp EEG was acquired using an EGI NA-400 amplifier (Electrical Geodesics, Inc; Oregon, USA) with a 256-channel Geodesic Sensor Net. SEEG activity was recorded simultaneously using a Nihon-Kohden Neurofax-1200 amplifier with DixiMedical intracerebral electrodes. Both signals were sampled at 1000 Hz.

The hdEEG net was placed on the head by trained neurosurgeons using sterile technique, following a precise step-by-step protocol: (1) sterilization of the net, (2) removal of the protective bandage from the subject's head, (3) skin disinfection with Betadine and Clorexan, (4) positioning of the hdEEG net, and (5) reduction of the impedances below 25–50 kOhm using conductive gel, (6) skin disinfection after net removal[58,59]. The electrical stimulator sent trigger signals recorded by the SEEG and hdEEG recordings, thus allowing for a precise synchronization of their traces. Scalp electrodes were initially referenced to Cz. SEEG electrodes were referenced online to a neutral couple of intracerebral contacts located in unresponsive white matter. Each SEEG electrode consisted of a variable number of contacts (between 18 and 5), with a contact length of 1.5 mm, diameter of 0.8 mm and intercontact spacing of 2 mm. The total number of contacts per subject was 197.5 ± 25.5. Electrode localization was performed by co-registering post-implantation computed tomography with pre-implantation structural magnetic resonance as in Mikulan et al (2020).

Preprocessing of simultaneous EEG and SEEG recordings. Signal preprocessing was performed in Python using MNE-Python [33]. Continuous SEEG data were filtered between 0.1 and 195 Hz using a zero-phase FIR filter with a Hamming window and automatically determined transition bandwidth. Continuous HdEEG data were filtered between 0.5 and 40 Hz using the same filtering approach. Line noise was attenuated using notch filters at 50 Hz and harmonics (100, 150, and 200 Hz). Epochs of both SEEG and

hdEEG were extracted from − 0.2 to 0.5 s relative to stimulus onset and baseline corrected in the interval − 0.2 to − 0.05 s.

Bad scalp channels were identified through visual inspection by trained neurophysiologists. These channels were excluded temporarily and subsequently reconstructed using spherical-spline interpolation[60].

Scalp EEG signals were transformed onto a standard 64-channel BioSemi montage. This harmonization step was performed using spline spatial interpolation interpolation and was required to obtain a common sensor representation across participants and across the independent datasets acquired with different EEG systems. The electrical stimulation artifact was attenuated using a custom median-based correction applied to a 25 ms interval centred on stimulus onset (as in Mikulan et al). Baseline correction was performed using the interval from − 0.2 to − 0.05 s. For model fitting, signals were normalized using the trial-specific prestimulus baseline. For SEEG data only, in addition to baseline mean subtraction, the signal was divided by the baseline standard deviation (z-score).

Trials containing residual stimulation artifacts, epileptiform discharges, amplifier saturation, or excessive physiological noise were rejected using the AutoReject algorithm[61] with default parameters, followed by manual inspection and rejection of residual artifacts. The mean number of retained trials was 485 ± 166 per session.

Identification of tonic-responsive intracranial contacts. The intracranial target was derived from SEEG contacts showing a sustained response following median nerve stimulation. Broadband gamma activity was estimated in the 50–150 Hz range by averaging the power obtained from Morlet wavelet decomposition computed at 10-Hz intervals, using a variable number of cycles equal to one-fifth of the corresponding frequency (i.e., frequency/5). Channels exhibiting tonic responses were identified using a k-means clustering algorithm as previously described by Avanzini et al. (2016). Gamma activity was normalized relative to the prestimulus interval from − 200 to − 20 ms and expressed as z-score. A contact was defined as tonic responsive when it showed a statistically significant post-stimulus increase in gamma activity satisfying the following criteria: binwise t-test, bonferroni corrected, significance threshold of p = 0.01 and a minimum duration of 20 ms (see Avanzini et al 2016 for details).

Contacts located within the seizure-onset zone, exhibiting frequent interictal epileptiform discharges, or showing persistent artifacts were excluded before response classification. Tonic-responsive contacts were identified using the K-Means procedure described by Avanzini et al. (2016). For each session, the tonic-responsive contact showing the largest gamma response was selected, and its gamma activity was used as the intracranial tonic-response waveform. This waveform constituted the target variable for model training.

Trial aggregation and generation of pseudo-trials. To improve the signal-to-noise ratio while preserving within-session variability, model inputs and targets were constructed using repeated random trial averages. For each recording session, 50 trials were randomly sampled with replacement and averaged.

The corresponding scalp EEG and intracranial target signals were averaged using identical trial indices. This procedure was repeated ten times, generating ten pseudo-trials for each session and 100 pseudo-trials across the complete simultaneous-recording dataset.

All pseudo-trials generated from the same participant were assigned to the same cross-validation fold. Thus, no pseudo-trial derived from a held-out participant contributed to model fitting.

Alignment of stimulation sides. To obtain a common anatomical representation across sessions, recordings acquired during right median nerve stimulation were mirrored across the sagittal plane. Scalp electrode labels and coordinates were exchanged between homologous left- and right-hemisphere positions. SEEG contact coordinates were similarly mirrored along the left–right axis. Following this transformation, all recordings were represented as if stimulation had occurred on the same side of the body. This procedure preserved the distinction between ipsilateral and contralateral activity while allowing a single model to be trained across stimulation sides.

Time-delayed ridge-regression model

Model definition. A time-delayed ridge-regression model was implemented using the ReceptiveField and TimeDelayingRidge functions available in MNE-Python[33–35]. The model estimated a linear transformation between the distributed scalp EEG signal and the intracranial tonic-response waveform. Time-shifted versions of each scalp EEG channel were included as predictors, allowing the model to capture temporal dependencies between scalp and intracranial activity.

Let Xc(t) denote the scalp EEG activity recorded at channel *c* and time *t*. The predicted intracranial tonic response was modeled as a linear mapping from scalp EEG activity (predictors) to the intracranial tonic response (target) by incorporating time-lagged versions of the input signals. Specifically, EEG recordings from 64 scalp channels were transformed into a set of lagged features by including temporally shifted copies of each channel within a predefined temporal window $[t_{min}, t_{max}]$. This formulation allows the model to capture the temporal relationships between scalp EEG activity and intracranial tonic responses (Fig. 1a).

Hyperparameter optimization. The regularization parameter (alpha) was explored over a logarithmically spaced range from (10^{-3}) to (10^{3}).

Candidate temporal windows were constructed by combining minimum lags of − 30, −20, − 10 and 0 ms with maximum lags of 30, 40, 50 and 60 ms.

For each combination of (alpha), minimum lag and maximum lag, model performance was evaluated using leave-one-subject-out cross-validation. At each fold, all sessions and pseudo-trials belonging to one participant were excluded from the training set and used exclusively for testing. Predicted and observed intracranial responses were compared within an evaluation interval extending from 60 ms plus the selected minimum lag to 250 ms plus the selected maximum lag. Performance was quantified as the

maximum Pearson cross-correlation between the predicted and observed intracranial tonic-response waveforms within a temporal displacement window of ± 50 ms. This procedure accommodated modest individual differences in response latency. Performance was summarized at two levels. (1) Pseudo-trial-level performance was defined as the median correlation between predicted and observed waveforms across all held-out pseudo-trials; (2) participant-level performance was defined as the median correlation between predicted and observed waveforms after aggregating predictions within each held-out participant. The hyperparameter combination maximizing median cross-validated performance across subjects was selected as the final model. The final model was selected based on the hyperparameter combination achieving the highest median performance across subjects in a leave-one-subject-out cross-validation framework. Following hyperparameter selection, the final model was fitted using all pseudo-trials from the simultaneous hdEEG-SEEG dataset and the selected model parameters. The fitted model was subsequently applied, without further adaptation, to the pooled perceptual-threshold and wake–sleep scalp EEG datasets. Before model application, all independent EEG datasets were transformed onto the same 64-channel montage, preprocessing pipeline and signal normalization used for model training.

Sensor-space representation of model coefficients. To describe the scalp distribution contributing to the reconstruction, model coefficients were averaged across temporal delays within the selected model window, yielding one summary coefficient for each of the 64 EEG channels. The resulting sensor-level distribution was projected onto the standard BioSemi montage. Because regression coefficients are influenced by the covariance structure of the predictors[38], they were interpreted as a description of the information used by the model rather than as a direct estimate of the cortical generators of the intracranial response.

Perceptual-threshold dataset

Participants and recording sites. The perceptual-threshold dataset combined recordings acquired independently at two research centres, Milan and Turin.

Both cohorts comprised eight participants each, resulting in a final pooled sample of 16 participants. Participants had no history of neurological or psychiatric disease. All participants provided written informed consent. The studies were approved by the local ethics committees at Local Ethical committees (Milan: Prot.n. 609/07/27/05/AP, Comitato Etico Milano Area 1; Turin: Prot.n. 0133259 of 20/02/2024, Comitato di Bioetica di Atene of the University of Turin).

Data acquisition for perceptual-threshold dataset. At both centres, the individual perceptual threshold was determined before the main experiment.

Median nerve stimulation intensity was adjusted to identify the current at which participants reported detecting five of ten consecutive stimuli. Experimental stimulation was subsequently delivered at the perceptual threshold plus an individual increment of 5–10%. This increment was selected to minimize

habituation to repeated stimulation and thereby obtain sufficient numbers of both perceived and unperceived responses while maintaining constant physical stimulation across conditions. Participants received 250 single-pulse stimulations of the median nerve at the wrist using a Digitimer DS7A constant-current stimulator. Each stimulus had a duration of 0.2 ms. Upon each trial, participants fixated a blank screen for a jittered pre-stimulus interval of 1.5 s (jitter range: ±0.25 s). Then, a stimulus was delivered, followed by a 0.5 post-stimulus interval. Immediately after, a visual cue prompted participants to indicate by button press whether they had perceived the somatosensory stimulus. The visual cue remained on screen until response, for a maximum of 1s. Trials were classified as perceived or unperceived according to the participant's report. The mean number of perceived trials was 121/250 in Milan, 108/250 in Turin, and 115/250 in the pooled dataset.

EEG acquisition. In Milan, scalp EEG was recorded using a 64-channel EEG system (BrainAmp DC, Brain Products GmbH, Germany) with a 10–10 montage layout cap. Data were collected at 1000 Hz sampling rate, at 0.5 μV amplitude resolution and with a hardware filtering bandwidth from DC to 250 Hz.

The online reference and ground electrodes were located over the frontal forehead. Additionally, bipolar electroculogram (EOG) was recorded in a diagonal montage. Electrode impedances were maintained below 10k Ohm.

Stimulus presentation, event timing, and behavioural responses were controlled and recorded using E-Prime 3.0 (Psychology Software Tools, Sharpsburg, PA, USA). Trigger markers were sent to the EEG acquisition system via a Chronos response device (Psychology Software Tools) to ensure precise synchronization between stimulus delivery and electrophysiological recordings.

Along the same line, in Turin, scalp EEG was recorded using a 64-channel ActiCHamp EEG system at a sampling frequency of 1000 Hz.

The online reference PoZ, and hardware filters were set from DC to 280 Hz. Electrode impedances were maintained below 10k Ohm.

Stimulus presentation, event timing, and behavioural responses were controlled and recorded using a custom-made combined E-Prime 3.0 (Psychology Software Tools, Sharpsburg, PA, USA) and Arduino (www.arduino.cc) script. Specifically, the E-Prime script coordinated the experimental timeline, by i) displaying the appropriate screens on the PC positioned in front of the participant (50 cm), ii) sending triggers to the Arduino board, which prompted the delivery of the tactile stimulus through the Digitimer High Voltage Stimulator (model DS7A), iii) sending triggers to the EEG system time-locked to tactile stimuli delivery, and iv) recording the participants' behavioural response.

Although the experimental paradigm was comparable across centres, the acquisition systems and recording environments differed. Pooling the two cohorts therefore introduced realistic between-site variability into the dataset used to derive SET*.

Preprocessing of perceptual-threshold EEG data. Data from the two centres were preprocessed using a common pipeline matched as closely as possible to that used for the simultaneous hdEEG-SEEG recordings. Continuous EEG was filtered between 0.5 and 40 Hz using a zero-phase, third-order Butterworth IIR band-pass filter. Line noise was attenuated using an FIR notch filter at harmonics of the power-line frequency (50, 100, 150, 200, and 250 Hz). Bad channels were identified by visual inspection by trained neurophysiologists and reconstructed using spherical-spline interpolation[60]. Data were re-referenced to the average of all good channels.

The stimulation artifact was corrected using a local spline interpolation approach applied within a 25 ms window around the stimulation onset, with a Tukey window used to smoothly blend the interpolated signal with the original data.

Epochs were extracted from − 200 to 500 ms relative to stimulus onset and baseline corrected using the interval from − 200 to − 20 ms.

Trials containing residual artifacts were rejected. The retained trials were separated into perceived and unperceived conditions.

For each participant, condition-specific EEG responses were obtained by averaging all retained trials classified as perceived or unperceived.

Before model application, EEG signals from both centres were interpolated onto the same standard 64-channel BioSemi montage used for model training. Signals were normalized relative to the prestimulus baseline using the same procedure applied to the simultaneous dataset.

N140/SAN quantification

The N140/SAN was quantified at the C6 electrode as a conventional scalp EEG benchmark. When necessary, scalp EEG recordings were left–right mirrored to align all data to a common stimulation side, ensuring that C6 was contralateral to the stimulated nerve. The latency window of the response considered was derived from a cluster-based permutation analysis[62]; Fig. 2). The most negative sample within this interval was identified separately for each participant and condition. N140/SAN amplitude was defined as the mean voltage within a ± 5-ms interval centred on the negative peak.

Scalp Estimated Tonicity

Application of the trained time-delayed ridge-regression model to a scalp EEG response generated a time-resolved estimate of intracranial tonic activity. To reduce the contribution of predicted fluctuations that were not distinguishable from prestimulus variability, SET quantification included only values of the estimated waveform exceeding twice the standard deviation of the baseline computed between − 0.2 and − 0.02 s. This criterion was applied identically across all participants, conditions, and datasets. Then, SET was defined as the area under the curve of predicted waveform values exceeding 2STD of the

baseline between 0.06 and 0.25 s after stimulation. This time window was selected to exclude early responses and to maximise the probability of detecting tonic responses[27]. At each time point, values not exceeding the criterion were set to zero, whereas the remaining amplitudes were summed over time while accounting for the sampling interval. SET therefore incorporated both the amplitude and temporal persistence of the predicted response above prestimulus variability.

Definition of the participant-level SET decision threshold (SET*)

The pooled Milan–Turin perceptual dataset was used to derive a single participant-independent SET decision threshold, denoted SET*, for separating perceived from unperceived condition averages. For each participant, one SET value was obtained from the perceived condition and one from the unperceived condition, yielding 32 participant-condition observations. Candidate thresholds spanning the observed range of SET values were evaluated, and SET* was defined as the threshold that maximized classification accuracy across these observations. SET values equal to or greater than SET* were classified as indicating the presence of predicted tonic activity, whereas values below SET* were classified as indicating its absence. This procedure yielded SET* = 6, which maximized accuracy, sensitivity and specificity in the pooled perceptual dataset. The same fixed threshold was then applied, without recalibration, to the independent wake–sleep dataset to assess its generalizability across brain states.

Wake–sleep dataset

Participants. The wake–sleep dataset comprised 8 participants. Participants had no history of neurological (including sleep disorders) or psychiatric disease. All provided written informed consent. The protocol was approved by the Ethics Committee of Milano Area 1 (prot. N°609/07/05/OA).

Median nerve stimulation during wakefulness and sleep. Participants underwent continuous median nerve stimulation during quiet wakefulness and sleep. Stimuli consisted of constant-current pulses with a duration of 0.2 ms, delivered to the right median nerve at the wrist. Stimulation intensity was set to 110% of the individual motor threshold and was therefore substantially above the perceptual threshold. During wakefulness, participants were eyes open and were instructed to rest relaxed on the chair. No trial-by-trial perceptual report was collected because stimulation was expected to be clearly perceptible at the selected intensity. During sleep, stimulation was delivered during N3 sleep, requiring slow-wave activity at 0.5–2 Hz with peak-to-peak amplitude > 75 μV over frontal derivations for at least 20% of a 30-s epoch, based on AASM sleep scoring criteria [63]. Stimuli associated with an electrophysiological arousal or awakening were excluded. A total of 258 ± 67 wake trials and 199 ± 59 N3 trials per participant were retained.

EEG acquisition and preprocessing. EEG was recorded using a 62-channel BrainAmp amplifier (Brain Products GmbH, Gilching, Germany). Signals were referenced to an additional forehead electrode, band-pass filtered between 0.016 and 1000 Hz, and digitized at a sampling rate of 5000 Hz (0.5 μV/bit

resolution). Electrode impedances were maintained below 10 kΩ throughout the recordings. Electrooculographic (EOG) activity was simultaneously recorded using two additional electrodes to monitor eye movements and blinks. Somatosensory stimulation was delivered using a constant-current stimulator (DS7A, Digitimer Ltd., Hertfordshire, UK). Bipolar transcutaneous electrical stimulation was applied at the wrist using monophasic square-wave pulses of 200 μs duration, with an inter-stimulus interval randomly jittered between 2.0 and 2.3 s. Stimulation intensity was individually adjusted to reliably elicit a visible thumb twitch without causing discomfort.

Preprocessing followed the same general procedures used for the perceptual-threshold datasets. Data were filtered, epoched, baseline corrected and cleaned of stimulation and physiological artifacts. Condition-specific responses were obtained by averaging retained wake and N3 trials separately. The trained model was then applied to the wake and sleep condition averages. Estimated waveforms and SET values were calculated using the same quantification procedure employed in the perceptual-threshold dataset. SET* = 6, previously derived from the pooled perceptual dataset, was then applied without recalibration.

Statistical analysis

Statistical analyses were performed in Python (version 3.12) using the SciPy library (version 1.14.1)[64]. All statistical tests were two-sided unless otherwise specified. Statistical significance was defined as ($p < 0.05$).

Model-prediction performance. Within each leave-one-subject-out fold, the predicted and observed intracranial response waveforms were compared using Pearson cross-correlation. Prediction performance was summarized using the median and interquartile range because the distribution of correlation coefficients was not assumed to be Gaussian. Performance was reported separately at the pseudo-trial and participant levels.

Cluster-based permutation analysis of perceived and unperceived scalp responses. To establish whether the conventional scalp response differentiated perceived from unperceived stimuli at the group level, a non-parametric cluster-based permutation analysis was performed on the pooled perceptual-threshold dataset [62]. For each participant, the unperceived condition average was subtracted from the perceived condition average at electrode C6. The resulting within-participant difference waveform was tested against zero. At each time sample within the post-stimulus interval from 0.06 to 0.25 s, a one-sample t statistic was calculated across participants. Temporally adjacent samples exceeding an initial threshold corresponding to a one-tailed $p < 0.05$ ($t = -1.753$, df = 15) were grouped into clusters. Cluster mass was defined as the sum of the t statistics within each temporal cluster. A null distribution was generated using 1000 random sign permutations of the participant-level difference waveforms. For each permutation, the maximum absolute cluster mass was retained. The corrected p value of an observed cluster was calculated as the proportion of permuted maximum cluster statistics equal to or greater than the observed statistic. Clusters were considered significant at a cluster-corrected threshold of ($p < 0.05$).

Group-level comparisons of SET and N140. Within-participant differences between perceived and unperceived conditions were tested separately for SET and N140 amplitude using Wilcoxon signed-rank tests. The same procedure was used to compare wakefulness and N3 sleep. Non-parametric tests were selected because of the small sample sizes and the distribution of the measures. Effect sizes were quantified using Cohen's (d_z), calculated as the mean paired difference divided by the standard deviation of paired differences. For N140 amplitudes, effect direction was defined such that a more negative response in the perceived or wake condition corresponded to a positive effect size.

Participant-level classification. In the pooled perceptual dataset, SET values were classified using SET*, which was estimated from the same dataset by maximizing classification accuracy. Classification performance was summarized using accuracy, sensitivity, and specificity. Because SET* was both derived and evaluated in the pooled perceptual dataset, these metrics were interpreted as measures of development-set separation. In the wake–sleep dataset, the same fixed SET* was used to classify wake and sleep condition averages. No model retraining, threshold recalibration, or modification of the SET quantification procedure was performed.

Effect of the number of EEG trials on prediction performance. To assess the robustness of the model with respect to the number of scalp EEG trials available per participant, we repeated the prediction analysis after selecting different numbers of EEG epochs with the highest signal-to-noise ratio (SNR) from each recording. For each participant and condition, subsets ranging from 5 to 65 epochs were retained. The same trained Time-Delayed Ridge model was then applied to each subset, and the predicted intracranial tonic response was quantified using the SET. For each subsampling level, classification accuracy for discriminating between perceived and unperceived stimulation was computed across participants.

Declarations

Consent to participate.

Written informed consent to participate in the study was obtained from all participants in accordance with the procedures approved by the relevant institutional ethics committees.

Competing interests.

The authors declare no competing interests.

Author Contributions

Conceptualization: E.P.M., A.P.; Methodology: E.P.M.; Data curation/collection: A.Ca., F.M., E.P.M., A.R.S., A.Co., G.H., F.M.Z., M.D.V., I.S., P.A., F.G., A.P.; Formal analysis: A.Ca., F.M.; Writing – original draft: A.Ca.,

F.M., A.P.; Writing – review & editing: A.Ca., F.M., P.A., F.G., A.P.; Supervision: A.P.; Funding acquisition: P.A., F.G., A.P. All authors read and approved the final version of the manuscript.

ACKNOWLEDGMENTS

This research was funded by the Progetto Di Ricerca Di Rilevante Interesse Nazionale (PRIN, P2022FMK77), Ministry of University and Research (MUR); by the Italian National Recovery and Resilience Plan (NRRP), M4C2, funded by the European Union - NextGenerationEU (Project IR0000011, CUP B51E22000150006, “EBRAINS-Italy”); by the Italian Ministry of Health through funding from Ricerca Corrente 2026 (2025–2027); by the European Research Council HORIZON-INFRA-2022 SERV (Grant No.101147319), "EBRAINS 2.0: A Research Infrastructure to Advance Neuroscience and Brain Health"; and by the European Research Council (ERC-2022-STG – 101078497 - MYFIRSTBODY; ERC-2022-SYG – 101071900 - NEMESIS).

Data availability.

The data supporting the findings of this study are available from the corresponding author upon reasonable request. Because the datasets include human intracranial electrophysiological recordings and associated clinical information, raw individual-level data cannot be made publicly available due to participant privacy and ethical restrictions. Requests for access to de-identified data will be evaluated in accordance with the relevant institutional ethics approvals and data-protection requirements.

Code Availability.

Code used in the present study is available at https://github.com/Framan99/TDR_algorithm/tree/main

References

1. Monti MM et al (2010) Willful modulation of brain activity in disorders of consciousness. N Engl J Med 362:579–589
2. King JR et al (2013) Single-trial decoding of auditory novelty responses facilitates the detection of residual consciousness. NeuroImage 83:726–738
3. Sitt JD et al (2014) Large scale screening of neural signatures of consciousness in patients in a vegetative or minimally conscious state. Brain J Neurol 137:2258–2270
4. Comanducci A et al (2020) Clinical and advanced neurophysiology in the prognostic and diagnostic evaluation of disorders of consciousness: review of an IFCN-endorsed expert group. Clin Neurophysiol Off J Int Fed Clin Neurophysiol 131:2736–2765
5. Sergent C, Baillet S, Dehaene S (2005) Timing of the brain events underlying access to consciousness during the attentional blink. Nat Neurosci 8:1391–1400

6. Del Cul A, Baillet S, Dehaene S (2007) Brain dynamics underlying the nonlinear threshold for access to consciousness. PLoS Biol 5:e260
7. Palva JM, Palva S, Kaila K (2005) Phase synchrony among neuronal oscillations in the human cortex. J Neurosci Off J Soc Neurosci 25:3962–3972
8. Sanz-Sánchez I et al (2020) Efficacy of access flap procedures compared to subgingival debridement in the treatment of periodontitis. A systematic review and meta-analysis. J Clin Periodontol 47:282–302
9. Fisch L et al (2009) Neural Ignition: Enhanced Activation Linked to Perceptual Awareness in Human Ventral Stream Visual Cortex. Neuron 64:562–574
10. Gaillard R et al (2009) Converging intracranial markers of conscious access. PLoS Biol 7:e61
11. Cogitate Consortium et al (2025) Adversarial testing of global neuronal workspace and integrated information theories of consciousness. Nature 642:133–142
12. Parvizi J, Kastner S (2018) Promises and limitations of human intracranial electroencephalography. Nat Neurosci 21:474–483
13. Mercier MR et al (2022) Advances in human intracranial electroencephalography research, guidelines and good practices. NeuroImage 260:119438
14. Koch C, Massimini M, Boly M, Tononi G (2016) Neural correlates of consciousness: progress and problems. Nat Rev Neurosci 17:307–321
15. Stockart F et al (2026) Neural correlates of perceptual consciousness from within: a narrative review of human intracranial research. Preprint at. https://doi.org/10.7554/eLife.109604.1
16. Tsuchiya N, Wilke M, Frässle S, Lamme VAF (2015) No-Report Paradigms: Extracting the True Neural Correlates of Consciousness. Trends Cogn Sci 19:757–770
17. Overgaard M, Fazekas P (2016) Can No-Report Paradigms Extract True Correlates of Consciousness? Trends Cogn Sci 20:241–242
18. Desmedt JE, Tomberg C (1989) Mapping early somatosensory evoked potentials in selective attention: critical evaluation of control conditions used for titrating by difference the cognitive P30, P40, P100 and N140. Electroencephalogr Clin Neurophysiol 74:321–346
19. Allison T, McCarthy G, Wood CC (1992) The relationship between human long-latency somatosensory evoked potentials recorded from the cortical surface and from the scalp. Electroencephalogr Clin Neurophysiol 84:301–314
20. Schubert R, Blankenburg F, Lemm S, Villringer A, Curio G (2006) Now you feel it–now you don't: ERP correlates of somatosensory awareness. Psychophysiology 43:31–40
21. Dembski C, Koch C, Pitts M (2021) Perceptual awareness negativity: a physiological correlate of sensory consciousness. Trends Cogn Sci 25:660–670
22. Auksztulewicz R, Spitzer B, Blankenburg F (2012) Recurrent Neural Processing and Somatosensory Awareness. J Neurosci 32:799–805

23. Schröder P, Nierhaus T, Blankenburg F (2021) Dissociating perceptual awareness and postperceptual processing: The P300 is not a reliable marker of somatosensory target detection. J Neurosci 41:4686–4696
24. Giorgi A et al (2025) Task Relevance Modulates Somatosensory Awareness Depending on Stimulus Intensity. Eur J Neurosci 62:e70262
25. Boly M et al (2007) Baseline brain activity fluctuations predict somatosensory perception in humans. *Proc. Natl. Acad. Sci.* 104, 12187–12192
26. Klostermann F et al (2009) Thalamo-cortical processing of near-threshold somatosensory stimuli in humans. Eur J Neurosci 30:1815–1822
27. Avanzini P et al (2016) Four-dimensional maps of the human somatosensory system. *Proc. Natl. Acad. Sci.* 113, E1936–E1943
28. Del Vecchio M et al (2019) Ipsilateral somatosensory responses in humans: the tonic activity of SII and posterior insular cortex. Brain Struct Funct 224:9–18
29. Albertini D et al (2025) Conscious tactile perception entails distinct neural dynamics within somatosensory areas. Curr Biol 35:2583–2596e3
30. Pigorini A et al (2024) Simultaneous invasive and non-invasive recordings in humans: A novel Rosetta stone for deciphering brain activity. J Neurosci Methods 408:110160
31. Antoniades A et al (2018) Deep Neural Architectures for Mapping Scalp to Intracranial EEG. Int J Neural Syst 28:1850009
32. Subramanian AK et al (2025) Scalp EEG predicts intracranial brain activity in humans. Preprint at. https://doi.org/10.1101/2025.04.07.647612
33. Gramfort A et al (2014) MNE software for processing MEG and EEG data. NeuroImage 86:446–460
34. Crosse MJ, Di Liberto GM, Bednar A, Lalor EC (2016) The Multivariate Temporal Response Function (mTRF) Toolbox: A MATLAB Toolbox for Relating Neural Signals to Continuous Stimuli. Front Hum Neurosci 10:604
35. Holdgraf CR et al (2017) Encoding and Decoding Models in Cognitive Electrophysiology. Front Syst Neurosci 11:61
36. Hogendoorn H, Kammers M, Haggard P, Verstraten F (2015) Self-touch modulates the somatosensory evoked P100. Exp Brain Res 233:2845–2858
37. Lio G, Boulinguez PH (2018) Does Sensor-Space Group Blind Source Separation Face Inter-individual Neuroanatomical Variability? Insights from a Simulation Study Based on the PALS-B12 Atlas. Brain Topogr 31:62–75
38. Haufe S et al (2014) On the interpretation of weight vectors of linear models in multivariate neuroimaging. NeuroImage 87:96–110
39. Toker D et al (2026) Adversarial AI reveals mechanisms and treatments for disorders of consciousness. Nat Neurosci 29:964–977

40. Xu L et al (2020) Cross-Dataset Variability Problem in EEG Decoding With Deep Learning. Front Hum Neurosci 14
41. Windt JM, Nielsen T, Thompson E (2016) Does Consciousness Disappear in Dreamless Sleep? Trends Cogn Sci 20:871–882
42. Siclari F et al (2017) The neural correlates of dreaming. Nat Neurosci 20:872–878
43. Riedner BA et al (2007) Sleep homeostasis and cortical synchronization: III. A high-density EEG study of sleep slow waves in humans. Sleep 30:1643–1657
44. Usami K et al (2015) Sleep modulates cortical connectivity and excitability in humans: Direct evidence from neural activity induced by single-pulse electrical stimulation. Hum Brain Mapp 36:4714–4729
45. Lendner JD et al (2020) An electrophysiological marker of arousal level in humans. eLife 9:e55092
46. von Ellenrieder N et al (2020) How the Human Brain Sleeps: Direct Cortical Recordings of Normal Brain Activity. Ann Neurol 87:289–301
47. Bekinschtein TA et al (2009) Neural signature of the conscious processing of auditory regularities. *Proc. Natl. Acad. Sci. U. S. A.* 106, 1672–1677
48. Polich J (2007) Updating P300: an integrative theory of P3a and P3b. Clin Neurophysiol Off J Int Fed Clin Neurophysiol 118:2128–2148
49. Kotchoubey B (2017) Evoked and event-related potentials in disorders of consciousness: A quantitative review. Conscious Cogn 54:155–167
50. Garrido MI, Kilner JM, Stephan KE, Friston KJ (2009) The mismatch negativity: a review of underlying mechanisms. Clin Neurophysiol Off J Int Fed Clin Neurophysiol 120:453–463
51. Dykstra AR, Gutschalk A (2015) Does the mismatch negativity operate on a consciously accessible memory trace? Sci Adv 1:e1500677
52. Casali AG et al (2013) A theoretically based index of consciousness independent of sensory processing and behavior. Sci Transl Med 5:198ra105
53. Casarotto S et al (2024) Dissociations between spontaneous electroencephalographic features and the perturbational complexity index in the minimally conscious state. Eur J Neurosci 59:934–947
54. Stender J et al (2014) Diagnostic precision of PET imaging and functional MRI in disorders of consciousness: a clinical validation study. Lancet 384:514–522
55. Bodart O et al (2017) Measures of metabolism and complexity in the brain of patients with disorders of consciousness. NeuroImage Clin 14:354–362
56. Kahane P, Landré E, Minotti L, Francione S, Ryvlin P (2006) The Bancaud and Talairach view on the epileptogenic zone: a working hypothesis. Epileptic Disord Int Epilepsy J Videotape 8(Suppl 2):S16–26
57. Cardinale F et al (2013) Stereoelectroencephalography: surgical methodology, safety, and stereotactic application accuracy in 500 procedures. *Neurosurgery* 72, 353–366; discussion 366

58. Mikulan E et al (2020) Simultaneous human intracerebral stimulation and HD-EEG, ground-truth for source localization methods. Sci Data 7:127
59. Parmigiani S et al (2022) Simultaneous stereo-EEG and high-density scalp EEG recordings to study the effects of intracerebral stimulation parameters. Brain Stimulat 15:664–675
60. Perrin F, Pernier J, Bertrand O, Echallier JF (1989) Spherical splines for scalp potential and current density mapping. Electroencephalogr Clin Neurophysiol 72:184–187
61. Jas M, Engemann DA, Bekhti Y, Raimondo F, Gramfort A, Autoreject (2017) Automated artifact rejection for MEG and EEG data. NeuroImage 159:417–429
62. Maris E, Oostenveld R (2007) Nonparametric statistical testing of EEG- and MEG-data. J Neurosci Methods 164:177–190
63. Berry RB et al (2017) AASM Scoring Manual Updates for 2017 (Version 2.4). J Clin Sleep Med JCSM Off Publ Am Acad Sleep Med 13:665–666
64. Virtanen P et al (2020) SciPy 1.0: fundamental algorithms for scientific computing in Python. Nat Methods 17:261–272

Figures

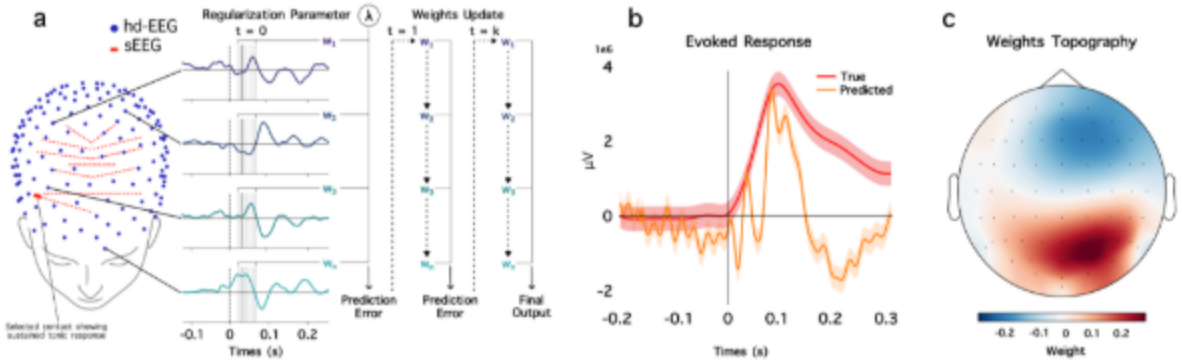


Figure 1

Performance and spatial weights of the scalp EEG-based time-delayed ridge model.

(a) Schematic of the recording setup and of the Time-Delayed Ridge model (see methods). **(b)** Comparison between observed and predicted tonic responses across subjects (mean ± SEM), together with the median maximum cross-correlation across pseudo-trials from held-out participants (0.67) and the median participant-level correlation (0.61). **(c)** Topographical distribution of Time-Delayed Ridge model weights from the temporal window selected for the final model (0-40 ms), averaged across temporal lags and projected onto sensor space using a 64-channel BioSemi EEG montage.

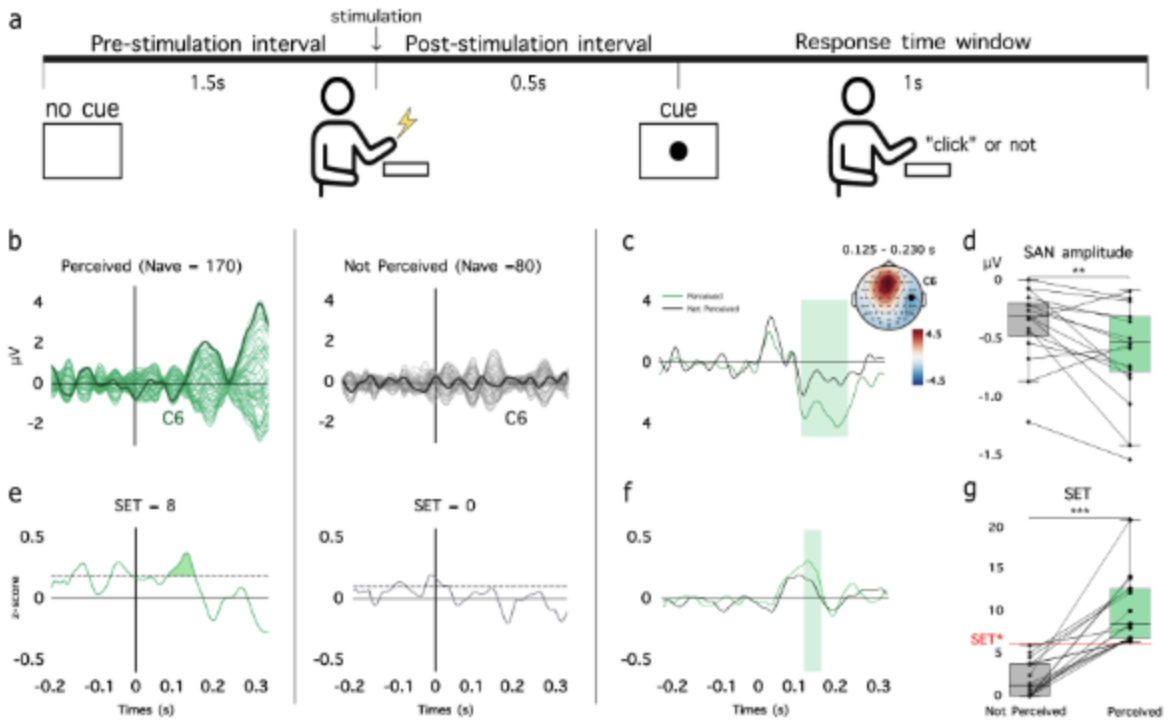


Figure 2

SET provide improved discrimination compared with the conventional SAN response and achieve participant-level separation at the somatosensory perceptual threshold.

(a) Schematic representation of the somatosensory perceptual-threshold paradigm. Participants received 250 constant-intensity median nerve stimuli set close to their individual perceptual threshold. Each trial comprised a jittered prestimulus interval (1.5 ± 0.25 s), median nerve stimulation, a 0.5-s post-stimulus interval, and a visual cue prompting a perceived/unperceived response. **(b)** Single-participant example of scalp EEG responses (Nave indicates the number of trials averaged per condition) to perceived and unperceived stimuli, with channel C6 highlighted in black. **(c)**One-sample cluster-based permutation test (PCT) performed on the within-participant difference waveforms at channel C6. A significant negative cluster was identified between 0.125 and 0.230 s after stimulation, corresponding to the N140 component and highlighted in light green. The top-right panel shows the scalp distribution of the perceived-minus-unperceived difference averaged across the significant temporal cluster, revealing the expected contralateral frontocentral negativity centred over electrode C6. **(d)**Comparison of SAN amplitude between perceived and unperceived conditions. At the group level, SAN amplitude was significantly larger, i.e. more negative, for perceived than for unperceived stimuli (**p < 0.01). **(e)**Representative examples of the tonic responses predicted for the perceived and unperceived conditions, corresponding to the scalp EEG signals shown in panel B. Scalp Estimated Tonicity (SET) was quantified between 60 and 250 ms as the time integral of estimated waveform exceeding a predefined baseline-exceedance criterion of 2 × σbaseline, indicated by the dashed line. **(f)** One-sample cluster-based permutation test performed on the within-participant difference between the estimated waveforms obtained for perceived and unperceived conditions. **(g)** Comparison of SET values between

perceived and unperceived conditions. At the group level, SET was significantly higher for perceived than for unperceived stimuli (**p < 0.01). The SET decision threshold derived from the pooled perceptual dataset (SET = 6; red dashed line) achieved complete development-set separation between perceived and unperceived condition averages (accuracy = 1).

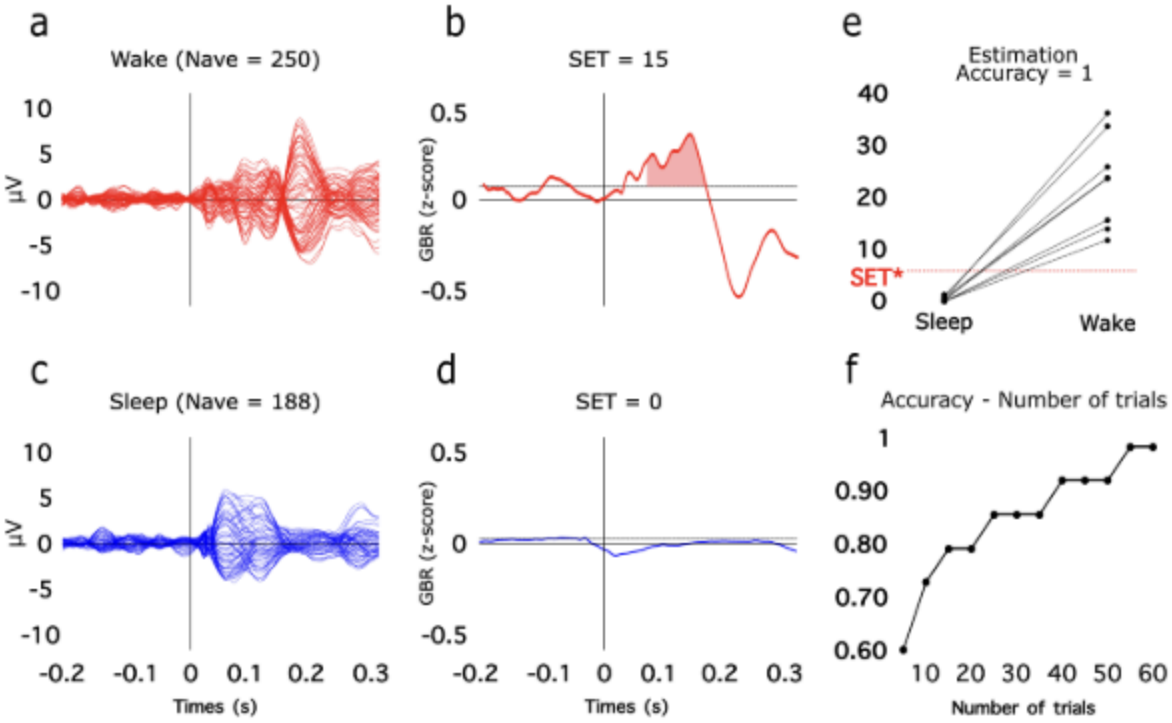


Figure 3

SET* generalizes to participant-level wake–sleep discrimination.

(a) Scalp EEG responses recorded during wakefulness (Nave = 250) in one representative subject. **(b)** Corresponding estimated scalp activity, yielding a SET value of 15. **(c)** Scalp EEG responses recorded during sleep (Nave = 188) in the same subject of (a). **(d)** Corresponding estimated scalp activity, yielding a lower SET value of 0. **(e)** Comparison of SET values between wakefulness and sleep. SET* (red-dashed line), derived from the independent perceptual-threshold dataset and applied without recalibration, is shown by the red dashed line. All wake-condition averages and sleep-condition averages were correctly classified, yielding an overall accuracy of 1. **(f)** Classification accuracy as a function of the number of trials included in the averaged EEG response.

Supplementary Files

This is a list of supplementary files associated with this preprint. Click to download.

- CalcagnoManniniSI.docx
- CalcagnoManniniSI.docx